SCHOOL OF ECONOMICS AND MANAGEMENT
FACULTY OF SOCIAL SCIENCES
AARHUS UNIVERSITY

CREATES
Center for Research in Econometric Analysis of Time Series

CREATES Research Paper 2009-30

Long Memory and Tail dependence in Trading Volume and Volatility

Eduardo Rossi and Paolo Santucci de Magistris

School of Economics and Management
Aarhus University
Bartholins Allé 10, Building 1322, DK-8000 Aarhus C
Denmark

Long Memory and Tail dependence in Trading Volume and Volatility †

Eduardo Rossi ‡ Paolo Santucci de Magistris §

July 13, 2009

Abstract

This paper investigates long-run dependencies of volatility and volume, supposing that are driven by the same informative process. Log-realized volatility and log-volume are characterized by upper and lower tail dependence, where the positive tail dependence is mainly due to the jump component. The possibility that volume and volatility are driven by a common fractionally integrated stochastic trend, as the *Mixture Distribution Hypothesis* prescribes, is rejected. We model the two series with a bivariate Fractionally Integrated VAR specification. The joint density is parameterized by means of with different copula functions, which provide flexibility in modeling the dependence in the extremes and are computationally convenient. Finally, we present a simulation exercise to validate the model.

Keywords. Realized Volatility, Trading Volume, Fractional Cointegration, Tail dependence, Copula Modeling. **J.E.L. classification.** C32, G12.

†We thank Dean Fantazzini who participated in an initial stage of this work.

‡Dipartimento di economia politica e metodi quantitativi, Via San Felice 5, University of Pavia, Italy. Corresponding author. Tel.: +39 0382/986207 Fax: +39 0382/304226. *E-mail address*: erossi@eco.unipv. Financial support from PRIN 2006 is gratefully acknowledged.

§Dipartimento di economia politica e metodi quantitativi, University of Pavia, Italy. Santucci de Magistris gratefullly acknowledges the kind hospitality of CREATES, funded by the Danish National Research Foundation, during the period September 2008 - April 2009.

1 Introduction

An extensive empirical literature has focused, during the last decades, on the temporal dependencies between volume and volatility on financial markets. The investigation of the volatility-volume relationship has important implications in terms of microstructure of financial markets. Numerous empirical investigations find a positive and strong contemporaneous correlation between both absolute returns and volume. One explanation for the positive price volatility-volume correlation is provided by the sequential information model, see Copeland (1975). In this model, the information is disseminated to only one trader at time and intermediate equilibria occur prior than the final equilibrium. Sequential information imply that there is a positive correlation between price volatility and trading volume in a sequential manner. In the simplest version of the *Mixture Distribution Hypothesis* (MDH, hereafter), see Clark (1973) and Epps and Epps (1976), price volatility and volume should be positively correlated because the joint dependence on a common underlying variable, that is interpreted as the rate of information flow. According to this theory, the dynamics of volume and volatility are driven by a common and contemporaneous informative process and both *bad news* and *good news* are accompanied by above average volume and volatility. However, this informative process is unobservable.

Given the leptokurtic distribution of daily returns the MDH implies that data are generated by a conditional stochastic process with variance parameter that varies over time. In particular, MDH helps to explain the high degree of positive correlation between volume and volatility (see Karpoff (1987)).

The literature on MDH can be classified in two groups. The first one focuses on estimation of the model parameters and latent variables to evaluate the goodness of fit with respect to real data.[1] The second one concentrates on the properties of the

[1] See the approach presented in Andersen (1996) and Liesenfeld (2001).

observed series, relying on an observable measure of volatility, see Bollerslev and Jubinski (1999) and Luu and Martens (2003). In the Bollerslev and Jubinski (1999) version of MDH, volume and volatility are supposed to be driven by an informative common process with long memory, while the short run dynamics are not necessarily the same. The authors interpret the MDH as a long run phenomenon in which the information arrival process is persistent. The main purpose of this paper is to model the relationship between volume and volatility where both are supposed to be driven by an unobserved long memory process (as in Bollerslev and Jubinski (1999)). To this end we use the realized volatility (as in Luu and Martens (2003)), computed from the intraday squared returns, which is a consistent estimator of the true daily integrated volatility. The results of the Nielsen and Shimotsu (2007) test support the idea that the two variables share the same order of long-range dependence. However, if this finding is supportive of the theory of MDH, at least in the version of Bollerslev and Jubinski (1999), it is not enough. In fact, if the two series were driven by the same long memory latent process, we would expect that there exists a linear combination that dampens the long run dependence. Thus we investigate the possibility that volume and realized volatility are fractionally cointegrated. The evidence of the Nielsen and Shimotsu (2007) test for fractional cointegration does not support this conclusion. This suggests that we can model the relationship between the logarithm of realized volatility and volume by a long memory bivariate model, that is a Fractionally Integrated VAR (FIVAR), which excludes the possibility of fractional cointegration.

One element that is important for the modeling of the long-run dependencies of volume and volatility is the tail dependence. The estimates of tail dependence of the filtered series suggest that a careful treatment of this aspect is needed. This naturally calls for a suitable choice of the joint distribution. We adopt different copulae functions to characterize the multivariate distribution function. Copulae provide a flexible tool to model dependence when only marginal distributions are known, but also allow for different tail dependencies.

A simulation exercise is carried out in order to evaluate the ability of the bivariate FIVAR model, with different copulae specifications, to account for some sample statistics. The benchmark model is a bivariate extension of the Heterogeneous Autoregressive (HAR) model introduced by Corsi (2009). The results are in favor of the FIVAR specification coupled with a joint density modeled as a mixture of copulae densities. The evidence from the estimation and simulation results highlight the ability of the FIVAR to account for the common long memory pattern that is observed in the data.

This paper is organized as follows. Section 2 briefly reviews the theoretical framework besides the concept of realized volatility and its decomposition. In Section 3 a brief description of the data appears. Section 4 investigates the long memory property of volatility and volume. In Section 5 tail dependence analysis is carried out. Section 6 sets up the model for volume and volatility. Section 7 presents the copulae modeling, while Section 8 reports the estimation results. Section 9 describes the simulation study for the validation of the model, and Section 10 concludes.

2 Realized variation and its decomposition

Let assume that the log-price, p_t, follows a continuous-time semimartingale process,

$$p_t = \int_0^t \mu_s ds + \int_0^t \sigma_s dW_s + \sum_{j=1}^{Q(s)} k(s_j), \tag{1}$$

where the mean process μ_t is continuous and of finite variation, $\sigma_t > 0$ denotes, as usual, the cad-lag instantaneous volatility. $Q(t)$ is a counting process that takes value 1 if a jump occurs at t, while $k(t)$ refers to its magnitude. The quadratic variation process is given by

$$[p]_t = p\lim\sum_{j=1}^{t_j<t}(p_{t_j}-p_{t_{j-1}})^2 = \int_0^t \sigma_s^2 \mathrm{d}s + \sum_{j=1}^{Q(s)} k^2(s_j) = IV_t + \sum_{j=1}^{Q(s)} k^2(s_j), \qquad (2)$$

where the *integrated volatility*, for day t, is defined as the integral of the spot volatility

$$IV_t = \int_{t-1}^{t} \sigma_s^2 \mathrm{d}s. \qquad (3)$$

When the jumps are present, the quadratic variation is equal to the sum of integrated volatility plus the jumps. The quadratic variation can be estimated by the sum of the intraday squared returns, $r_{t_j}^2$, i.e. the realized volatility,

$$RV_t = \sum_{j=1}^{M}(p_{t_j}-p_{t_{j-1}})^2 = \sum_{j=1}^{M} r_{t_j}^2 \quad t = 1,...,T \qquad (4)$$

where M is the number of intraday observations. The realized volatility converges to the integrated volatility plus the jump component.

However, prices sampled at high frequency are affected by the so called microstructure bias and the estimation of integrated volatility becomes imprecise. This fact has been analyzed and solved in different ways (see Ait-Sahalia and A. Mykland (2003), Hansen and Lunde (2006) and Bandi and Russell (2006)). The simplest way to deal with this problem is sampling at lower frequencies (for example 5 minutes as in Corsi et al. (2005) or Bollerslev et al. (2009)).

Barndorff-Nielsen and Shephard (2004), have shown that RV allows for a direct nonparametric decomposition of the total price variation into its two separate components: a continuous part, called *Bipower Variation* (*BPV*), and a discontinuous one, the *Jumps*. Incorporating a measure of jumps is important because, as it has been noted by Huang and Tauchen (2003), their relative contribution to the total price variability is about 7%. The *BPV* is defined as

$$BPV_t = \frac{\pi}{2} \sum_{j=2}^{M} |r_{t,j}||r_{t,j-1}| \quad t = 1, ..., T \tag{5}$$

and converges to IV_t as M diverges.

Corsi et al. (2008) show that the apparent puzzle found in Andersen et al. (2007), where the jumps seem to not have forecast ability for the future volatility is due to a measurement bias, introduced by the bipower variation in finite samples. In fact, suppose $r_{t,j}$ contains a jump. In the case of bipower variation, it will multiply two adjacent returns, $r_{t,j-1}$ and $r_{t,j+1}$. As M increases, both these returns will vanish and bipower variation will converge to integrated continuous volatility. But when M is finite, these returns will not vanish, causing a positive bias which will be larger as $r_{t,j}$ increases. This consideration suggests that the bias of bipower variation will be extremely large in case of consecutive jumps. This causes a positive bias when the bipower variation is used to account for the continuous part of volatility, in particular when two jumps occur in the same daily trajectory.

Mancini (2007) proposes an alternative method for identifying the continuous part of realized volatility based on the following truncation:

$$TRV_t = \sum_{j=1}^{M} r_{t,j}^2 \cdot I(|r_{t,j}| < \theta), \tag{6}$$

where θ is a threshold function. This method will throw out more returns as jumps during a high volatility period than during a low volatility period.

Corsi et al. (2008) provide an alternative estimator of the continuous part of volatility, the *Corrected Threshold Bipower Variation*, hence after $CTBPV$, that is

$$CTBPV_t = \frac{\pi}{2} \sum_{j=2}^{M} Z_1(r_{t,j}, \theta_j) Z_1(r_{t,j-1}, \theta_{j-1}) \quad t = 1, ..., T \tag{7}$$

where $Z_1(r_{t,j}, \theta_j)$ is a special function equal to $|r_{t,j}|$ when $r_{t,j} < \theta_j$, and equal to $1.094\sqrt{\theta_j}$ when $r_{t,j} \geq \theta_j$, and θ_j is the threshold that is a multiple of local variance, $\hat{V}_j$, that is chosen according to an iterative procedure, so that

$$\theta_j = c_\theta \cdot \hat{V}_j.$$

The residual jump component is then calculated as the difference between the realized volatility and the $CTBPV$

$$J_t = RV_t - CTBPV_t \quad t = 1, ..., T. \tag{8}$$

3 Data

Our data set consists of 5-minutes IBM transaction prices from January 1, 1995 through December 31, 2003. Returns, $r_{i,t}$, over five minutes interval are then calculated, and realized volatility is obtained as the sum of 81 intraday squared returns over five minutes intervals. Daily volume are given by the sum of intraday volume.[2]

The series consists of 2267 daily observations. BPV_t and J_t are obtained as in formulas (5) and (8). As it is apparent from Figure 1. the logarithm of volume and realized volatility are clustered. There is no graphical evidence of the presence of a strong time trend. However, we fit a quadratic trend and consider for the subsequent analysis the detrended series.[3] The Box-Pierce portmanteau test statistic (in Table 1) shows that volatility and volume are highly autocorrelated, while re-

[2]The total number of observations is 183627. The raw data are the *tick-by-tick* prices and volume on IBM relative to the open market (from 9:30 am to 4:15 pm). Using the method of *previous tick*, the series of prices over a grid of five minutes have been created, as well the volume, as the sum of the number of transactions since the last interval. Week-end and festivity are excluded from the database to avoid seasonality effects.

[3]In the rest of the paper, we refer to $\log RV_t$, $\log BPV_t$, $\log CTBPV_t$ and $\log V_t$ as the detrended versions of the corresponding measures. These are obtained simply regressing log-volatilities and log-volume on a constant, a time trend and a squared time trend.

turns and J_t are much less persistent. Moreover, the continuous part of volatility ($\log CTBPV$) is more persistent than realized volatility, since the jumps, which is the non persistent component, has been disentangled.

4 The MDH as a Long Memory Relationship

There is accordance in the literature (Andersen et al. (2003), Corsi et al. (2005) and Bollerslev et al. (2009)) on some stylized facts:

- the distribution of realized volatility is asymmetric and leptokurtic, but the density of logarithm of the series is nearly Gaussian.
- both volatility and volume seems to be long memory. This means that the effect of a shock decays slowly. This fact is in contrast with an ARMA representation (which implies an exponential decay) or a unit root process.

Long memory is defined in terms of decay rates of long-lag autocorrelations, or in the frequency domain in terms of rates of explosion of low frequency spectra. A long-lag autocorrelation definition of long memory is

$$\gamma(\tau) = c_\gamma \tau^{2d-1} \quad \tau \to \infty,$$

where $c_\gamma > 0$, τ is the lag and d is the long memory parameter. It is evident that the autocorrelations of long memory processes decay with a hyperbolic rate and they are not summable. An alternative, although not equivalent, definition of long range dependence can be given by using the spectral density $f(\lambda)$ of the process:

$$\lim_{\lambda \to 0^+} \frac{f(\lambda)}{c_f |\lambda|^{-2d}} = 1 \quad 0 < c_f < \infty.$$

The spectral density $f(\lambda)$ has a pole and behaves like a constant c_f times λ^{-2d} at the origin. If $|d| \in (0, 1/2)$ the process is stationary. In particular, if $d \in (0, 1/2)$, it presents long memory; instead, if $d \in (-1/2, 0)$ the process is antipersitent with short memory. A popular approach to the modeling of long memory is represented by the ARFIMA class introduced by Granger and Joyeux (1980) and Hosking (1981). They generalize the class of ARIMA models by allowing a fractional degree of differencing.

Lieberman and Phillips (2008) provides an analytical explanation for the evidence of long memory in the series of realized volatility. In fact, the autocovariance structure of the realized volatility estimator depends on those of the intraday returns. Then, even if the intraday increments are short memory, the sampling scheme renders the RV to be long memory. This suggest that the latent information arrival process, that is approximated by the realized volatility, should also have long memory, since it is the sum of independent intraday information arrivals.

Bollerslev and Jubinski (1999) investigate the nature of the common aggregate latent information-arrival process, postulated by the MDH. They assume that this common latent process is characterized by long-range persistence. They test the equality of fractional integration degree of absolute returns for each of the 100 individual shares in the Standard and Poor's 100 composite index and the corresponding volume, finding, in general, a common long-run hyperbolic decay rate.

Luu and Martens (2003) extend previous analysis considering the realized volatility as a proxy of the volatility of IBM and modeling volume and volatility using a VAR, finding bidirectional Granger causality. Fleming and Kirby (2006), examine the long-run relationship between volatility and volume in a bivariate Fractional VAR, that is a VAR on the fractionally differenced series. Their results indicate that volume and realized volatility generally display the same degree of fractional integration, suggesting that the main source of time variation is found in their long memory property, while, differently from Luu and Martens (2003), a minor role is attributable to the VAR components.

Nevertheless, the equality of the fractional integration orders does not imply the validity of the MDH theory. In fact, if the MDH theory were verified, there should exist a common stochastic trend, that is the latent information arrival process with long memory, that drives the dynamics of both volatility and volume through time. Hence, the analysis of the validity of the MDH should be carried out investigating the degree of fractional cointegration of volume and volatility. In the next section, we shortly present the definition of fractional cointegration and we test for the MDH theory in the case of IBM data.

4.1 Fractional cointegration analysis

According to the definition in Granger (1986), two (or more) $I(d)$ series are fractionally cointegrated if there exists a linear combination that is $I(d_e)$, with $d_e < d$. Thus the errors are of lower order of fractional integration than the levels. This means that the series share fractionally integrated stochastic trends of different orders ($I(d)$ and $I(d_e)$), and a linear combination eliminates the largest. More precisely, suppose that z_t is a vector $(p \times 1)$ of observables, where the i-th element $z_{it} \sim I(d_i)$, with $d_i > 0$, $i = 1, \ldots, p$, we say that they are fractionally cointegrated if there exists a vector $\alpha \neq 0$

$$e_t = \alpha' z_t \equiv I(d_e) \quad 0 \leq d_e < \min_{1 \leq i \leq p} d_i.$$

This is possible if and only if $d_i = d_j$, some $i \neq j$; a necessary condition for α to be a cointegrating vector is that its i-th component be equal to zero if $d_i > d_j$ for all $i \neq j$. When $d_1 = \ldots = d_p = d$ it is usual to write $z_t \equiv CI(d, b)$, $b = d - d_e$. A typical situation is when $z_t = (x_t', y_t) \in I(d)$ and $e_t \in I(d_e)$ with $d > d_e \geq 0$ in the model

$$y_t = \beta' x_t + e_t. \tag{9}$$

Cointegration is commonly thought of as a stationary relation between nonstationary variables

$$d_i \geq \frac{1}{2} \quad \forall i \quad \text{and} \quad d_e < \frac{1}{2}.$$

But another possibility, which is relevant to the present analysis, is represented by $0 \leq d_i < \frac{1}{2} \forall i$, i.e. z_t and e_t are stationary. Thus the case where $d > 0$, $d_e \geq 0$ and $d + d_e \leq 1/2$ is called stationary fractional cointegration. The main drawback of fully specified parametric models is that they provide inconsistent estimators of the long-run parameters if the model is not correctly specified. The MDH prescribes *full* cointegration between volatility and volume, in the sense that $b = d$ or $d_e = 0$. Since the presence or absence of fractional cointegration is not known when testing for the equality of the fractional integration orders in a regression model, we rely on a testing procedure for $H_0 : d_{\log RV} = d_{\log V}$ that is informative in both circumstances. Robinson and Yajima (2002) discuss a semi-parametric procedure for determining the cointegration rank, focusing on stationary series, i.e. $d < 1/2$. Nielsen and Shimotsu (2007) extend the analysis of Robinson and Yajima (2002), in order to consider cointegration for both stationary and non-stationary variables. In particular, they apply the exact local Whittle analysis, and estimate the rank of spectral cointegration of the dth differenced process around the origin. The test statistic for the equality of integration orders in the bivariate case is

$$\widehat{T} = m(S\hat{d})' \left(S\frac{1}{4}\hat{D}^{-1}(\hat{G} \odot \hat{G})\hat{D}^{-1}S' + h(T)^2 \right)^{-1} (S\hat{d}), \tag{10}$$

where $\odot$ denotes the Hadamard product, $S = [1, -1]'$, $h(T) = \log(T)^{-k}$ for $k > 0$, $D = \text{diag}(G_{11}, G_{22})$, while $\hat{G} = \frac{1}{m}\sum_{j=1}^{m} Re(I_j)$ is a consistent estimator of $G = f_\epsilon(0)$

(see Nielsen and Shimotsu (2007) for more details). The vector of estimates $\widehat{d} = (\widehat{d}_{\log RV}, \widehat{d}_{\log V})$ is obtained with the univariate exact Whittle estimator developed by Shimotsu and Phillips (2005), that makes no assumptions on the presence of cointegration and is consistent in both cases.

If the variables are not cointegrated, that is the cointegration rank r is zero, $\widehat{T} \rightarrow \chi_1^2$, while if $r \geq 1$, $\widehat{T} \rightarrow 0$. A significantly large value of $\widehat{T}$, with respect to χ_1^2, can be taken as an evidence against the equality of the integration orders.

Moreover, the estimation of the cointegration rank r is obtained by calculating the eigenvalues of the estimated matrix $\hat{G}$. Table 2 shows the results of the Nielsen and Shimotsu (2007) fractional cointegration analysis, with two different choices for the bandwidths, m_d, used in the estimation of d, and m_L used in the estimation of $L(u)$. The null hypothesis that $r = 0$ cannot be rejected. This finding reinforces our belief against the idea of MDH theory as a long memory relationship. The estimated long memory parameters $(d_{\log RV}, d_{\log V})$ are in the stationary region. Moreover the $\widehat{T}$ statistic takes values 1.048 and 1.9716 which, in case of absence of cointegration, implies, as in Bollerslev and Jubinski (1999), the acceptance of the null hypothesis (we refer to the 95$\%$ critical value of a χ_1^2 that is 3.841), i.e the equality of the fractional differencing parameters.

5 Tail Dependence

Once the series of daily volatility and volume are obtained from intradaily data, it would be interesting to investigate the kind of dependence between the two series. The Pearson correlation measure only applies to observations that are not far out in the tails. The MDH does not provide an explanation for possible positive or negative upper/lower tail dependence. Nevertheless, the exploration of the extremal dependence structure, between volume and volatility, becomes fundamental for identifying and modeling their joint-tail dependence. Following Poon et al. (2004), we consider $\overline{\chi}$ as a measure of asymptotic dependence between volatility and volume, which assumes value 1 for asymptotically dependent variables. $\overline{\chi}$ is estimated with the Hill estimator, that is a non parametric measure of the degree of tail dependence,

$$\widehat{\overline{\chi}} = \frac{2}{n_u} \left(\sum_{j=1}^{n_u} \log \left(\frac{z_j}{u} \right) \right) - 1, \tag{11}$$

where n_u is the number of observation over the threshold u. z_j is the j-th order statistic from $Z = min(S, T)$, where S and T are the unit Frchet marginals of $\log RV$ and $\log V$,

$$S = -1/\log F(\log RV) \quad T = -1/\log F(\log V) \tag{12}$$

and $F(\cdot)$ is the univariate empirical distribution function. The variance of $\widehat{\overline{\chi}}$ is given by:

$$Var[\widehat{\overline{\chi}}] = \frac{(\widehat{\overline{\chi}} + 1)}{n_u}.$$

If there is evidence that $\widehat{\overline{\chi}} < 1$, $\widehat{\overline{\chi}} + 1.96\sqrt{Var[\widehat{\overline{\chi}}]} < 1$ then we can infer that the variables are asymptotically independent. Only if there is no significant evidence to reject $\bar{\chi} = 1$, we consider the degree of tail dependence, $\chi \in (0, 1)$, that is estimated by

$$\widehat{\chi} = \frac{u \cdot n_u}{T} \tag{13}$$

with variance,

$$Var[\widehat{\chi}] = \frac{u^2 n_u (T - n_u)}{T^3}.$$

The parameter χ measures the degree of upper tail dependence, that is the probability of observing a large value of volatility given a large realization of volume. The analysis of the lower tail dependence is symmetric to the right tail, since the data are multiplied by -1. Figures 2(a) and 2(b) report the calculated degree of tail dependence, $\widehat{\chi}$, between the series of volatility (including bipower variation, threshold realized volatility and corrected threshold-bipower variation) and $\log V$, for different choices of the threshold u. We repeat the tail dependence analysis on the filtered series, that is $(1-L)^{d_{RV}} \log RV, (1-L)^{d_V} \log V$, where the parameter d is estimated with the exact Whittle estimator, see Figure 2(c) and 2(d). Choosing a threshold u equal to 2.5% of observations, so that $n_u = 57$, the $\log V$ and $\log RV$ show left tail dependence, the same is true for the filtered series. For what concerns the right tail dependence, $\log RV$ and $\log BPV$ show positive dependence with $\log V$, in particular when the series are fractionally differenced. From the standard error expression is clear that decreasing u we increase the estimate uncertainty. The estimated degree of right tail dependence between $\log BPV$ and $\log V$, $\hat{\chi}$, is positive, $\hat{\chi} = 0.3306$, with 2.5% of observations on the right tail. $\log RV$ present a significant level of asymptotic upper and lower tail dependence with respect to log-volume. The estimated $\widehat{\chi}$ is equal to 0.3622 and 0.2904, with 2.5% of observations respectively on right and left tail, when considering the fractionally differenced series. Interestingly, we don't find the same evidence for the for the $\log CTBPV$. In fact, even if for $n_u = 57$ it shows asymptotic right tail dependence, the confidence band for the Hill estimator between $\log CTBPV$ and $\log V$ does not contain the value 1 in most cases. Moreover, the $\log TRV$ does not show right tail dependence, while behaves exactly as the $\log RV$ on the left tail. The $\widehat{\chi}$ in this case is positive and equal to 0.3245 and to 0.2904 when the series is fractionally differenced.

Figures 2(a) and 2(b) highlight three important features that characterize the relationship between volatility and volume.

- First, log-realized volatility and log-volume display positive upper and lower tail dependence. This means that, given an extreme positive value of volume, there is a positive probability (0.3989) to observe very high volatility the same day. There is also evidence of positive left tail dependence, i.e. when the trades are few, volatility and volume are asymptotically positively correlated.

- Second, the positive upper tail dependence is mainly due to the contribution of jumps to the realized volatility. In fact, $\log CTBPV$, that is the continuous part of realized volatility, and $\log V$ are asymptotically independent. This highlights the importance of a good estimation of the jump component of realized volatility. As noted by Corsi et al. (2008), the bipower variation underestimates the jump component, in particular in case of two consecutive jumps in the intradaily returns. Moreover, the $\log TRV$ well describes the continuous component of realized volatility when positive jumps occur, while seems to be unable to account for jumps with negative sign, that determine the level of left tail dependence.

- Third, the positive lower and upper tail dependence is not due to the long memory component. The positive tail dependence is still present after the fractional differencing.

6 The Model

Given the results of the fractional cointegration and tail dependence analysis, it is interesting to study the long run dependence of the two series and their interdependencies in a multivariate framework defined as a system of two equations:

$$\Phi(L)D(L)X_t = \epsilon_t \tag{14}$$

$$D(L) = \begin{bmatrix} (1-L)^{d_{rv}} & 0 \\ 0 & (1-L)^{d_v} \end{bmatrix}$$

where $X_t = (\log RV_t, \log V_t)'$, $\Phi(L) = I_2 - \Phi_1 L - ... - \Phi_p L^p$, $\epsilon_t = (\epsilon_{1t}, \epsilon_{2t})'$, with $E(\epsilon_t) = 0$ and $Var(\epsilon_t) = \Sigma$. This model is a Fractionally Integrated VAR (FIVAR).

Sowell (1989) develops an exact maximum likelihood procedure for the FIVAR estimation, with K series, based on the assumption that $X = (X_{1\cdot}, ..., X_{K\cdot})'$, where $X_{k\cdot} = (X_{k1}, \ldots, X_{kT})$, is a stationary multivariate Gaussian process. The unconditional Gaussian log-likelihood function is given by

$$\log L(\varphi|X) = -\frac{T}{2}\log(2\pi) - \frac{1}{2}\log(|\Gamma(\varphi)|) - \frac{1}{2}X'\Gamma(\varphi)^{-1}X$$

where $\Gamma(\varphi) = Cov(X)$ is the $KT \times KT$ matrix of the autocovariance of X, that depends on the vector of model's parameters φ. Sowell (1989) proposes an algorithm for computing the autocovariances of a FIVAR process, where $Cov(X_{i,t}, X_{j,t-s})$ are evaluated using the hypergeometric function, which has no closed form and is slow to compute. Following Bertelli and Caporin (2002), Sela and Hurvic (2008) propose to approximate the likelihood function writing the autocovariances as an infinite convolution between the covariances of an ARFIMA(0,d_k,0) and the infinite MA(∞) representation of a VAR process.

In this paper, we model the dependence structure between the volatility and volume in terms of copula function, deriving the likelihood from the infinite AR representation of the long memory processes. This means that, instead of modeling the autocovariance matrix for the entire sample path and then compute the Gaussian likelihood as in Sowell (1989), we maximize the conditional maximum likelihood function that considers a truncation of the infinite AR representation of a fractional process (see Beran (1994)). This estimation method allows for a flexible choice of the marginal distributions, where the instantaneous dependence structure between volatility and volume is determined by the choice of a copula function.

Following Beran (1994) and Palma (2007), both series are filtered by long memory, under the hypothesis that presample values are equal to zero. The infinite autoregressive representation of a fractional process, that is the best linear prediction of

X_t, is expanded to

$$(1-L)^{d_i} X_{i,t} = \sum_{j=0}^{t-1} \pi_{i,j} X_{i,t-j} \equiv \widetilde{Z}_{i,t} \quad i = 1, \ldots, K$$

where $\pi_0 = 1$, $\pi_1 = -d$, $\pi_j = \frac{1}{j}\pi_{j-1}(j-1-d)$ for $j \geq 2$. The model (14) can be rewritten as

$$\Phi(L)\widetilde{Z}_t = \epsilon_t \quad t = 1, \ldots, T.$$

Now we can compute the log-likelihood function for observation t as

$$\log L(\varphi|\widetilde{Z}_t) = -\frac{1}{2}\log(2\pi) - \frac{1}{2}\log(|\Sigma|) - \frac{1}{2}\widetilde{Z}_t'\Sigma^{-1}\widetilde{Z}_t.$$

As noted by Beran (1994), the infinite autoregressive representation is not restricted to the case where the endogenous variables are stationary, but it can be extended to any $d > -\frac{1}{2}$. The approximate conditional maximum likelihood estimator is therefore defined for any stationary and non stationary fractional process.

7 Copula Modeling and Marginals Estimation

We assume that the ϵ_t have a joint distribution $\epsilon_t \sim G(\epsilon_t; \psi)$, with $G(.)$ continuous density function. The vector $\psi = (\varphi, \nu)$ contains the parameters of the conditional mean, variances and covariance (φ) and the nuisance parameters (ν). We specify the joint multivariate density by means of a copula function density. The copula theory provides an easy way to deal with the (otherwise) complex multivariate modeling. The essential idea of the copula approach is that a joint distribution can be factorized into the marginals and a dependence function called copula. The joint distribution $G(\epsilon_{1,t}, \epsilon_{2,t}; \psi)$ can be expressed as follows, thanks to the so-called

Sklar's theorem (1959):

$$(\epsilon_{1,t}, \epsilon_{2,t})' \sim G\left(\epsilon_{1,t}, \epsilon_{2,t}; \psi\right) = C\left(F_{1,t}(\epsilon_{1,t}; \delta_1), F_{2,t}(\epsilon_{2,t}; \delta_2); \gamma\right) \tag{15}$$

that is the joint distribution $G(.)$ of a vector of innovations ϵ_t is the copula $C\left(\,\cdot\,;\gamma\right)$ of the cumulative distribution functions of the innovations marginals $F_{1,t}(\epsilon_{1,t};\delta_1)$ $F_{2,t}(\epsilon_{2,t};\delta_2)$, where $\gamma, \delta_1, \delta_2$ are the copula and marginals parameters, respectively. The copula couples the marginal distributions together in order to form a joint distribution. The dependence relationship is entirely determined by the copula, while scaling and shape (mean, standard deviation, skewness, and kurtosis) are determined by the marginals (see Sklar (1959), Joe (1997) and Nelsen (1999)). Copulae can therefore be used to obtain more realistic multivariate densities than the traditional joint normal one, which is simply the product of a normal copula and normal marginals. Marginals can be entirely general, e.g. Skewed Student's *t* marginals.[4] Let $\Theta = (\delta_1, \delta_2; \gamma)$ be the parameters vector to be estimated, where δ_i, $i = 1, 2$ are the parameters of the marginal distribution F_i and γ is the vector of the copula parameters. It follows from (15) that the log-likelihood function for the joint conditional distribution G is by

$$l(\Theta) = \sum_{t=1}^{T} \log(c(F_1(\epsilon_{1,t}; \delta_1), F_2(\epsilon_{2,t}; \delta_2); \gamma)) + \sum_{t=1}^{T} \sum_{i=1}^{2} \log f_i(\epsilon_{i,t}; \delta_{i,t}). \tag{16}$$

where c is the copula density, whereas f_i are the marginals densities. Hence, the log-likelihood of the joint distribution is just the sum of the log-likelihoods of the margins and the log-likelihood of the copula. Standard ML estimates may be obtained by maximizing the above expression with respect to the parameters $(\delta_1, \delta_2; \gamma)$. In practice this can involve a large numerical optimization problem with many parameters which can be difficult to solve. However, given the partitioning

[4]Appendix A reports the alternative copula functions used in the estimation of model 14.

of the parameter vector into separate parameters for each margin and parameters for the copula, one may use (16) to break up the optimization problem into several small optimizations, each with fewer parameters. This multi-step procedure is known as the method of Inference Functions for Margins (*IFM*), see Joe and Xu (1996) and Joe (1997). According to the IFM method, the parameters of the marginal distributions are estimated separately from the parameters of the copula. Joe (1997) compares the efficiency of the IFM method relative to full maximum likelihood for a number of multivariate models and finds the IFM method to be highly efficient. Therefore, we think it is safe to use the IFM method and benefit from the huge reduction in complexity it implies for the numerical optimization.
We then compute the marginal log-likelihoods, under the hypothesis that $\epsilon_{1,t}$ and $\epsilon_{2,t}$ are the skew-*t* distributed (see Azzalini and Capitanio (2003)). Skew-*t* distribution corresponds to the transformation

$$\epsilon_i = \mu_i + Z_i/\sqrt{V_i} \quad i = RV, V$$

where $Z \sim SkewN(0, \sigma_i^2, \xi_i)$ and $V_i \sim \chi^2_{\nu_i}/\nu_i$. Finally, the log-likelihood functions of the FIVAR are obtained according to the IFM method described above, for each choice of the copula function. Appendix B reports the log likelihood functions for each copula specification.

8 Estimation Results

The maximum likelihood estimates of $d_{\log RV}$ and $d_{\log V}$ are always close to the semiparametric estimates obtained with the exact local Whittle estimator. The R^2 are about 30% for both log-volume and log-volatility. The estimated parameters, ϕ_{ij}, turn out to be statistically significant in the equation of the realized volatility, meaning that lagged filtered log-volume give some information on the actual fil-

tered realized log-volatility. This indicates that, once the long memory of the series is accounted for, volume leads volatility. However, this finding contrasts the results in Luu and Martens (2003) that ascertain, in a VAR framework, a bidirectional Granger causality from realized volatility to volume and in the other way round[5].
The parameters ξ_{RV} and ξ_V capture the positive skewness of the two series, in particular of realized volatility. The copula estimates show a positive dependence: if we compute a common dependence measure - such as the Kendall's tau - by using the parameters' estimates, it ranges from 0.3477 obtained with the Clayton copula up to 0.4316 with the Normal copula. The three copulae differ on the degree of tail dependence, that is dependence in the extremes: the Gumbel estimates are characterized by a strong upper tail dependence (0.4956), whereas the t-copula presents a lower value (0.1456). Clayton copula shows a strong lower tail dependence equal to 0.5289. The tail dependence coefficient is zero for the normal copula by construction. In a recent large scale simulation study, Fantazzini (2008) found that if the true marginals show positive skewness, then using symmetric marginals causes the Clayton parameter α_c to be positively biased, thus overestimating the tail dependence coefficient.
These results are in accordance with the findings of the preliminary non parametric analysis which highlights positive upper and lower tail dependence. In particular, the tail dependence value associated with the t-copula model is very close to the one obtained with the Hill's estimator. Besides, Kole et al. (2007) by using a new goodness-of-fit testing procedure, found that the Gaussian copula underestimates the probability of joint extreme downward movements, while the survival Gumbel copula overestimates this risk, and they provide evidence in favor of the Student's t-copula.

[5]The Granger causality test, given a VAR(1) model for our series, results in the acceptance of causality in both directions at 5% of significance. This results is robust to different choices of the lags of the VAR.

Table 6 reports the results of the goodness of fit tests conducted on the pseudo series of the residuals of model in (14). All the tests highlight the fact that the Clayton copula is not a good choice for accounting the tail dependence between volatility and volume. This result is not surprising, since, as noted before the source of tail dependence are the jumps that affect the dependence on the right tail. On the other hand, there is a mixed evidence in favor of all the other copula specifications. In particular, when the Rosenblatt transform is applied to the marginals, we notice that the Gumbel copula reports the best result in terms of goodness-of-fit. The results of the copula goodness-of-fit tests in table suggest that a mixture of copulae could improve the fit, since it allows for asymmetric tail dependence. We consider two mixtures: the Clayton copula and its survivor function, CMC, and the Gumbel copula and its survivor function, CMG.[6] Table 4 shows that λ, the mixing parameter, is lower than 0.5 in both cases. This confirms a strong asymmetric tail dependence, since the dependence on the right tail between volatility and volume is higher than that on the left tail, reinforcing the impression that the t-copula performs poorly since it does not allow for asymmetric tail dependencies.

9 Model Simulations

So far, we have discussed the model estimation results in terms of goodness of fit and their interpretations in the copula framework. Now, by means of simulations, we evaluate the ability of each specification to account for the sample characteristics of the observed data (see Table 6(a) and 6(b)). As a benchmark provision, we adopt a bivariate extension of the Heterogeneous Autoregressive (HAR) model, introduced by Corsi (2009). This simple model emphasizes the idea of heterogeneity among different investors on the financial markets. For this reason, Corsi (2009) suggests that the volatility depends on the past daily, weekly and monthly real-

[6]More details on mixture of copula are presented in Appendix A.

izations. We also include the volume, so that the extended bivariate HAR model is

$$
\begin{aligned}
\log V_t &= \omega_1 + \delta_{11} \log RV_{t-1} + \delta_{12} \log RV^W_{t-1} + \delta_{13} \log RV^M_{t-1} + \psi_{11} \log V_{t-1} \\
&\quad + \psi_{12} \log V^W_{t-1} + \psi_{13} \log V^M_{t-1} + \eta_{1t} \\
\log RV_t &= \omega_2 + \delta_{21} \log RV_{t-1} + \delta_{22} \log RV^W_{t-1} + \delta_{23} \log RV^M_{t-1} + \psi_{21} \log V_{t-1} \\
&\quad + \psi_{22} \log V^W_{t-1} + \psi_{23} \log V^M_{t-1} + \eta_{2t}
\end{aligned}
$$

where $\log RV^W_{t-1} = \frac{1}{5}\sum_{i=1}^{5} \log RV_{t-i}$ and $\log RV^M_{t-1} = \frac{1}{22}\sum_{i=1}^{22} \log RV_{t-i}$, while $(\eta_{1t}, \eta_{2t})'$ is distributed as a bivariate normal with zero mean and variance and covariance matrix, Γ, and is estimated by maximum likelihood.

The simulation exercise is based on the generation of model innovations according to the different copula specifications. 4267 observations from the FIVAR specification are generated by our Monte Carlo exercise for each copula function, keeping only the last 2267 observations corresponding to the sample size of our data. The first 2000 simulated observations serve as a burn-in period. We also generate series from the Gaussian HAR introduced above. Then, we repeat this simulation exercise 1000 times, in order to obtain 1000 daily sample paths for the logarithmic volume and volatility. From the 1000 simulated path, we calculate the model-implied sample distribution for the respective descriptive statistics. Table 6(a) and 6(b) report the descriptive statistics of $\log RV$ and $\log V$, respectively, and the 95% simulated confidence intervals. We also report actual quantiles and simulated confidence interval.

For what concerns the log-realized volatility, nearly all of the sample statistics lie within the simulated confidence bands obtained with FIVAR coupled with copula densities. Moreover, for all copula models, the simulated confidence intervals include the sample skewness. The same is not true for the HAR model. Notice that the confidence intervals from the simulation of a bivariate HAR contain neither the upper nor the lower empirical quantiles. The results are better off in the case of $\log V$. Table 6(c) reports the confidence interval of for the Hill's estimator of the tail dependence, computed from the simulated series. It is evident that neither the Gaussian HAR nor the Normal copula are able to account for the tail dependence of the data. In fact, the 95% confidence interval of the $\bar{\chi}$ estimator does not contain the value 1. On the other hand, Clayton and Gumbel copula explain the positive tail dependence respectively on the left and right tail. In fact, the value 1 is contained in the confidence interval of $\bar{\chi}$, and the observed values of the tail dependence are included in the confidence interval of χ. It is worth noticing, the simulated data from the t-copula model do not mimic the degree of tail dependence of the observed series, and this could be explained by the fact that the estimated t-copula has a lower tail dependence. This finding is in accordance with the results of the goodness-of-fit tests for the t-copula. The results of the simulations from the model with mixtures of copulae are completely different. In Table 7(a), 7(b) the 95% confidence intervals obtained by simulation contains the sample statistics for both series. Even more interestingly it is the fact that the intervals obtained for $\overline{\chi}$ (Table 7(c)), with the mixture of Clayton, contain the value of 1 for both tails, and the same occurs for χ. This confirms that the model with Clayton mixture is able to reproduce left tail dependence and right tail dependence. We also explore the dynamic implications of the models, in terms of ability to account for the hyperbolic rate of decay of the autocorrelation functions. Figure 3 plots the sample autocorrelations and the corresponding simulated 95% confidence bands.[7] Our bivariate long memory models, for $\log RV_t$ and $\log V_t$, reproduce the highly significant and very slowly decaying of the sample autocorrelations over longer multi-month lags. These results show how our bivariate FIVAR well describes the dynamics of

[7]Figure 3 displays the simulated ACF confidence bands relative to the Clayton copula. The conclusion are the same with respect to alternative copula specifications.

both volumes and volatility. In fact, the long memory bivariate model is able to reproduce both the sample statistics and the long run dynamics of the observed data in particular when the joint distribution is described by a mixed copula function.

10 Conclusions

This paper has focused on the relation between volatility and volume. Thanks to the recent developments on high-frequency based realized volatility, the former can be estimated rather precisely from the high frequency returns. We disentangle the realized volatility in a continuous and jump component, showing that volume are highly correlated with the continuous part of volatility and that jumps are much less persistent than bipower variation and volume. We also show that there exist a strong upper and lower tail dependence between the volatility and volume that is due to the presence of jumps. We don't provide a specific model for jumps, but we investigate the long memory property of realized volatility and volume, showing that the two series have the same degree of fractional integration but they do not appear to be fractionally cointegrated, in the sense that a linear combination of them does not reduce the degree of fractional integration. This finding is not supportive of the presence of a common stochastic long memory informative process for both volume and volatility as in the MDH version of Bollerslev and Jubinski (1999). Given the results of the fractional cointegration analysis, we propose and estimate a bivariate FIVAR model for the volume and realized volatility. However, the tail dependence makes the Gaussian assumption inadequate and calls for different hypotheses about the joint multivariate density. To this end we model the joint density by means of copulae functions. This has also the advantage of simplifying the computation of the log-likelihood function, which is for the FIVAR model computationally intensive. The whole system is estimated with an efficient full information maximum likelihood technique adopting different copulae, which in turn imply different tail dependencies. We also provide evidence that the FIVAR model coupled with a mixture of copulae is able to account for the long run dynamics of both volatility and volume, and this is also confirmed by a simulation exercise.

A Copula Functions

The class of elliptical distributions allows to model multivariate extreme events and forms of non-normal dependencies. Elliptical copulae are simply the copulae of elliptical distributions (see Fang et al. (1990) for a detailed treatment of elliptical distributions).

1. The probability density function of the Gaussian copula is:

$$c(\Phi(x_1), \Phi(x_2)) = \frac{1}{|R|^{1/2}} \exp\left(-\frac{1}{2}\zeta'(R^{-1} - I)\zeta\right) \tag{17}$$

   where $\zeta = (\Phi^{-1}(u_1), \ldots, \Phi^{-1}(u_n))'$ is the vector of univariate normal inverse distribution functions, $u_i = \Phi\,(x_i)$, while R is the correlation matrix.

2. The density of the copula of the Student's t-*Copula*, and its density function is:

$$c(T_{\nu_c}(x_1), T_{\nu_c}(x_2)) = |R|^{-1/2} \frac{\Gamma\left(\frac{\nu_c+2}{2}\right)}{\Gamma\left(\frac{\nu_c}{2}\right)} \left[\frac{\Gamma\left(\frac{\nu_c}{2}\right)}{\Gamma\left(\frac{\nu_c+1}{2}\right)}\right]^2 \frac{\left(1 + \frac{\zeta'\Sigma^{-1}\zeta}{\nu_c}\right)^{-\frac{\nu_c+2}{2}}}{\prod_{i=1}^{2}\left(1 + \frac{\zeta_i^2}{\nu_c}\right)^{-\frac{\nu_c+1}{2}}} \tag{18}$$

   where $u_i = T_{\nu_c}(x_i)$ and $T_{\nu_c}(x_i)$ is the univariate Student's *t* cdf, $\zeta = (T_{\nu_c}^{-1}(u_1), T_{\nu_c}^{-1}(u_2))'$ is the vector of univariate inverse distribution functions, ν_c are the degrees of freedom, and R is the correlation matrix.

The Student's *t*-copula generates symmetric tail dependence, i.e. lower and upper tail dependence are equal, while the normal copula generates zero tail dependence, instead.

An alternative to the elliptical copulae is the class of *Archimedean copulae*. Archimedean copulae provide analytical tractability and a large spectrum of different dependence measures. The *Gumbel copula*:

$$C(u_1, u_2) = \exp\left\{- \left[(-\log u_1)^\theta + (-\log u_2)^\theta\right]^{\frac{1}{\theta}}\right\} \tag{19}$$

where $\theta > 1$ is the copula parameter, whereas the density is given by

$$\begin{aligned} c(u_1, u_2) &= C(u_1, u_2) \cdot u_1^{-1} u_2^{-1} \left[(-\log u_1)^\theta + (-\log u_2)^\theta\right]^{-2+2/\theta} \\ & [\log u_1 \log u_2]^{\theta-1} \times \left\{1 + (\theta - 1)[(-\log u_1)^\theta + (-\log u_2)^\theta]^{-\frac{1}{\theta}}\right\} \end{aligned}$$

The degree of upper tail dependence for the Gumbel copula is equal to $2 - 2^{\frac{1}{\theta}}$. This is a measure of dependence between random variables in the extreme upper joint tails. Broadly speaking, we can say that the upper tail dependence measures the probability of an extremely large positive realization in one covariate, given that we have observed a large positive realization in another.

We also use the *Clayton* (or *Cook Johnson*) *copula*, which corresponds to copula B4 in Joe (1997):

$$C(u_1, u_2) = \max\left[\left(\sum_{i=1}^{2} u_i^{-\alpha_c} - 1\right)^{-1/\alpha_c}, \quad 0\right]$$

when the copula parameter $\alpha_c > 0$ the copula simplifies to

$$C(u_1, u_2) = (u_1^{-\alpha_c} + u_2^{-\alpha_c} - 1)^{-1/\alpha_c} \tag{20}$$

whereas the density is given by

$$c(u_1, u_2) = (1 + \alpha_c)(u_1 u_2)^{-\alpha_c - 1}\left(\sum_{i=1}^{2} u_i^{-\alpha_c} - 1\right)^{-\frac{1}{\alpha_c} - 2}.$$

It has positive *lower* tail dependence. This is a measure of dependence between random variables in the extreme lower joint tails. The Clayton copula implies a degree of tail dependence equal to $2^{(-1/\alpha_c)}$. See Joe (1997) and Cherubini et al.

(2005) for more details.

Since a convex linear combinations of copula functions is a copula, see Nelsen (1999), we combine the Gumbel copula, $C_G(.)$, and the Clayton copula, $C_C(.)$, in the following way

$$C_{MG}(u_1, u_2) = \lambda C_G(v_1, v_2; \theta_l) + (1-\lambda) C_G(u_1, u_2; \theta_r) \tag{21}$$

$$C_{MC}(u_1, u_2) = \lambda C_C(u_1, u_2; \alpha_l) + (1-\lambda) C_C(v_1, v_2; \alpha_r) \tag{22}$$

in order to account for the possible presence of asymmetries between left and right tail dependence.

The parameter $0 < \lambda < 1$ is the mixing parameter while $\theta_l \neq \theta_r$, or $\alpha_l \neq \alpha_r$, reflects the possible asymmetries in the left and right tail dependence. The vectors $v_1 = 1 - u_1$ and $v_2 = 1 - u_2$ are the reciprocal of the transformed series u_1 and u_2.

B Log-likelihood Functions

The log-likelihood functions for each copula density are:

- NORMAL COPULA (*NCOP*):

$$\begin{aligned} l_t(\Theta) &= \sum_{i=1}^{2} \log \left(\frac{2}{\sigma_i} t_{\nu_i} \left(\frac{\epsilon_i - \mu_i}{\sigma_i}; 1, \nu_i \right) + T_{\nu_i} \left(\alpha_i \frac{\epsilon_i - \mu_i}{\sigma_i} \sqrt{\frac{\nu_i + 1}{\left(\frac{\epsilon_i - \mu_i}{\sigma_i}\right)^2 + \nu_i}}, 1, \nu_i + 1 \right) \right) \\ &+ \left(-\frac{1}{2}(1-\rho^2)^{-1}(\epsilon_{1,t}^2 + \epsilon_{2,t}^2 - 2\rho\epsilon_{1,t}\epsilon_{2,t}) \cdot \frac{1}{2}(\epsilon_{1,t}^2 + \epsilon_{2,t}^2) \right) \end{aligned}$$

  where $t_{\nu_i}(., 1, \nu)$ and $T_{\nu_i}(., 1, \nu)$ are respectively the pdf and cdf of the t distribution with ν degrees of freedom and scale equal to 1. The parameter α measures the degree of skewness, while μ and σ are the location and scale parameters respectively.

- CLAYTON COPULA (*CCOP*):

$$
\begin{aligned}
l_t(\Theta) &= \sum_{i=1}^{2} \log \left(\frac{2}{\sigma_i} t_{\nu_i} \left(\frac{\epsilon_i - \mu_i}{\sigma_i}; 1, \nu_i \right) + T_{\nu_i} \left(\alpha_i \frac{\epsilon_i - \mu_i}{\sigma_i} \sqrt{\frac{\nu_i + 1}{\left(\frac{\epsilon_i - \mu_i}{\sigma_i}\right)^2 + \nu_i}}, 1, \nu_i + 1 \right) \right) \\
&+ \log \left((1 + \alpha_c)(u_{1,t} u_{2,t})^{-\alpha_c - 1} (u_{1,t}^{-\alpha_c} + u_{2,t}^{-\alpha_c} - 1)^{-(2 + \alpha_c^{-1})} \right)
\end{aligned}
$$

- T-COPULA (*TCOP*):

$$
\begin{aligned}
l_t(\Theta) &= \sum_{i=1}^{2} \log \left(\frac{2}{\sigma_i} t_{\nu_i} \left(\frac{\epsilon_i - \mu_i}{\sigma_i}; 1, \nu_i \right) + T_{\nu_i} \left(\alpha_i \frac{\epsilon_i - \mu_i}{\sigma_i} \sqrt{\frac{\nu_i + 1}{\left(\frac{\epsilon_i - \mu_i}{\sigma_i}\right)^2 + \nu_i}}, 1, \nu_i + 1 \right) \right) \\
&+ \log \left(\frac{\Gamma\left(\frac{\nu_c + 2}{2}\right) \Gamma\left(\frac{\nu_c}{2}\right)}{\Gamma\left(\frac{\nu_c + 1}{2}\right)^2} \cdot |R|^{-\frac{1}{2}} \left(1 + \frac{\zeta_t' R^{-1} \zeta_t}{\nu_c} \right)^{-\frac{\nu_c + 2}{2}} \right) \\
&+ \sum_{i=1}^{2} \log \left(1 + \frac{\zeta_{it}^2}{\nu_c} \right)^{\left(\frac{\nu_c + 1}{2}\right)}
\end{aligned}
$$

- GUMBEL COPULA (*GCOP*):

$$
\begin{aligned}
l_t(\Theta) &= \sum_{i=1}^{2} \log \left(\frac{2}{\sigma_i} t_{\nu_i} \left(\frac{\epsilon_i - \mu_i}{\sigma_i}; 1, \nu_i \right) + T_{\nu_i} \left(\alpha_i \frac{\epsilon_i - \mu_i}{\sigma_i} \sqrt{\frac{\nu_i + 1}{\left(\frac{\epsilon_i - \mu_i}{\sigma_i}\right)^2 + \nu_i}}, 1, \nu_i + 1 \right) \right) \\
&+ \log \left(C(u_1, u_2) \cdot u_1^{-1} u_2^{-1} \left[(-\log u_1)^{\theta} + (-\log u_2)^{\theta} \right]^{-2 + 2/\theta} [\log u_1 \log u_2]^{\theta - 1} \right) \\
&+ \log \left\{ 1 + (\theta - 1) [(-\log u_1)^{\theta} + (-\log u_2)^{\theta}]^{-\frac{1}{\theta}} \right\}
\end{aligned}
$$

References

Ait-Sahalia, Y. and A. Mykland, P. (2003). How often to sample a continuous-time process in the presence of market microstructure noise. NBER Working Papers 9611, National Bureau of Economic Research, Inc.

Andersen, T. G. (1996). Return volatility and trading volume: An information flow interpretation of stochastic volatility. *Journal of Finance*, 51:169–203.

Andersen, T. G., Bollerslev, T., and Diebold, F. X. (2007). Roughing it up: Including jump components in the measurement, modeling and forecasting of return volatility. *Review of Economics and Statistics*, 89(4).

Andersen, T. G., Bollerslev, T., Diebold, F. X., and Labys, P. (2003). Modeling and forecasting realized volatility. *Econometrica*, 71:579–625.

Azzalini, A. and Capitanio, A. (2003). Distributions generated by perturbation of symmetry with emphasis on a multivariate skew t-distribution. *Journal of the Royal Statistical Society, Series B*, 65:367–389.

Bandi, F. and Russell, J. (2006). Separating market microstructure noise from volatility. *Journal of Financial Economics*, 73:655–692.

Barndorff-Nielsen, O. E. and Shephard, N. (2004). Power and bipower variation with stochastic volatility and jumps. *Journal of Financial Econometrics*, 2:1–37.

Beran, J. (1994). *Statistics for Long-Memory Processes*. Chapman & Hall.

Bertelli, S. and Caporin, M. (2002). A note on calculating autocovariances of long memory processes. *Journal of Time Series Analysis*, 23:503–508.

Bollerslev, T. and Jubinski, D. (1999). Equity trading volume and volatility: Latent information arrivals and common long-run dependencies. *Journal of Business & Economic Statistics*, Vol. 17:9–21.

Bollerslev, T., Kretschmer, U., Pigorsch, C., and Tauchen, G. E. (2009). A discrete-time model for daily s&p 500 returns and realized variations: Jumps and leverage effects. *Journal of Econometrics*, forthcoming.

Breymann, W., Dias, A., and Embrechts, P. (2003). Dependence structures for multivariate high-frequency data in finance. *Quantitative Finance*, 3:1 – 14.

Cherubini, U., Luciano, E., and Vecchiato, W. (2005). *Copula Methods in Finance*. Wiley and Sons Ltd.

Clark, P. (1973). A subodinated stochastic process model with finite variance for speculative prices. *Econometrica*, 41:135–155.

Copeland, T. (1975). A model of asset trading under the assumption of sequential information arrival. *Journal of Finance*, September:1149–1168.

Corsi, F. (2009). A simple approximate long-memory model of realized volatility. *Journal of Financial Econometrics*, 7:pp. 174–196,.

Corsi, F., Kretschmer, U., Mittnik, S., and Pigorsch, C. (2005). The volatility of realized volatility. CFS Working Paper Series 2005/33, Center for Financial Studies. available at http://ideas.repec.org/p/cfs/cfswop/wp200533.html.

Corsi, F., Pirino, D., and Ren, R. (2008). Volatility forecasting: the jumps do matter. Technical report, Quaderni del Dipartimento Di Economia Politica, Universit Degli Studi Di Siena.

Epps, T. and Epps, M. (1976). The stochastic dependence of security price changes and transaction volumes: Implications for the mixture distribution hypotesis. *Econometrica*, 44:305–321.

Fang, K. T., Kotz, S., and Ng, K. W. (1990). *Symmetric Multivariate and Related Distribution*. Chapman & Hall, London.

Fantazzini, D. (2008). The effects of misspecified marginals and copulas on computing the value at risk: A monte carlo study. *Computational Statistics and Data Analysis*, Article in Press.

Fleming, J. and Kirby, C. (2006). Long memory in volatility and trading volume. Technical report.

Genest, C., Remillard, B., and Beaudoin, D. (2007). Goodness-of-fit tests for copulas: A review and a power study. *Insurance: Mathematics and Economics*, doi:10.1016/j.insmatheco.2007.10.005.

Granger, C. W. J. (1986). Developments in the study of cointegrated economic variables. *Oxford Bulletin of Economics and Statistics*, 48(3):213–28.

Granger, C. W. J. and Joyeux, R. (1980). An introduction to long-memory time series models and fractional differencing. *Journal of Time Series Analysis*, 4:221–238.

Hansen, P. R. and Lunde, A. (2006). Realized variance and market microstructure noise. *Journal of Business & Economic Statistics*, 24:127–161.

Hosking, J. (1981). Fractional differencing. *Biometrika*, 68:165–76.

Huang, X. and Tauchen, G. (2003). The relative contribution of jumps to total price variance. Technical report, Department of Economics, Duke University,.

Joe, H. (1997). *Multivariate Models and Dependence Concepts*. Chapman & Hall, New York.

Joe, H. and Xu, J. (1996). The estimation method of inference functions for margins for multivariate models. Technical report, Technical Report no. 166, Department of Statistics, University of British Columbia.

Karpoff, J. M. (1987). The relation between price changes and trading volume: A survey. *Journal of Financial and Quantitative Analysis*, 22:109–123.

Kole, Koedijk, and Verbeek (2007). Selecting copulas for risk management. *Journal of Banking and Finance*, 31:2405–2423.

Lieberman, O. and Phillips, P. C. B. (2008). Refined inference on long-memory in realized volatility. *Econometric Reviews*, 27(1):254–267.

Liesenfeld, R. (2001). A generalized bivariate mixture model for stock price volatility and trading volume. *Journal of Econometrics*, 104:141–178.

Luu, J. C. and Martens, M. (2003). Testing the mixture-of-distrubutions hypotesis using "realized" volatility. *The Journal of Future Markets*, 7:661–679.

Mancini, C. (2007). Non-parametric threshold estimation for models with stochastic diffusion coefficient and jumps,. *Scandinavian Journal of Statistics*, Forthcoming.

Nelsen, R. (1999). *An Introduction to Copula*. Springer-Verlag.

Nielsen, M. . and Shimotsu, K. (2007). Determining the cointegration rank in nonstationary fractional system by the exact local whittle approach. *Journal of Econometrics*, 141:574–596.

Palma, W. (2007). *Long-Memory Time Series: Theory and Methods*. Publisher: Wiley-Interscience, Wiley Series in Probability and Statistics.

Poon, S., Rockinger, M., and Tawn, J. (2004). Extreme value dependence in financial markets: Diagnostics, models, and financial implications. *Review of Financial Studies*, 17(2):581–610.

Robinson, P. M. and Yajima, Y. (2002). Determination of cointegrating rank in fractional systems. *Journal of Econometrics*, 106:217–241.

Sela, R. J. and Hurvic, C. M. (2008). Computationally efficient gaussian maximum likelihood methods for vector arfima models. Technical report, New York University.

Shimotsu, K. and Phillips, P. C. (2005). Exact local whittle estimation of fractional integration. *Annals of Statistics*, 33(4):1890–1933.

Sklar (1959). Fonctions de repartition a n dimensions et leurs marges. Technical report, Publications de l'Institut de Statistique de L'Universit de Paris.

Sowell, F. (1989). Maximum likelihood estimation of fractionally integrated time series models. Technical report, unpublished manuscript Carnegie-Mellon University.

	ρ_1	ρ_5	ρ_{10}	ρ_{40}	$BP(5)$	$BP(10)$	$BP(40)$
r_t	-0.0158	-0.0425	0.0242	0.0199	5.94	12.49	54.74
$\log RV_t$	0.5638	0.3633	0.2826	0.0891	2260.1^a	3318.3^a	5756.1^a
$\log BPV_t$	0.5870	0.3856	0.3083	0.1053	2482.6^a	3673.2^a	6370.7^a
$\log TVR_t$	0.5800	0.3799	0.2994	0.0962	2411.9^a	3594.0^a	6305.8^a
$\log CTBPV_t$	0.5875	0.4035	0.3369	0.1482	2633.7^a	4006.3^a	7643.6^a
J_t	0.0628	0.0116	-0.0033	-0.0101	13.56^b	15.19	27.83
$\log V_t$	0.6108	0.2879	0.2221	0.0608	2023.6^a	2591.2^a	3684.0^a

Table 1: Table reports the sample autocorrelation function (ρ_j), the Box-Pierce Portmanteau test statistic (BP) for 5, 10 and 40 lags of log-realized volatility ($\log RV_t$), log-bipower variation ($\log BPV_t$), log-threshold realized volatility ($\log TRV_t$), log corrected threshold bipower variation ($\log CTBPV_t$), jump component (J_t) and log-volume ($\log V_t$). *a*,*b* and *c* stands for 1%, 5% and 10% significance level of the BP test.

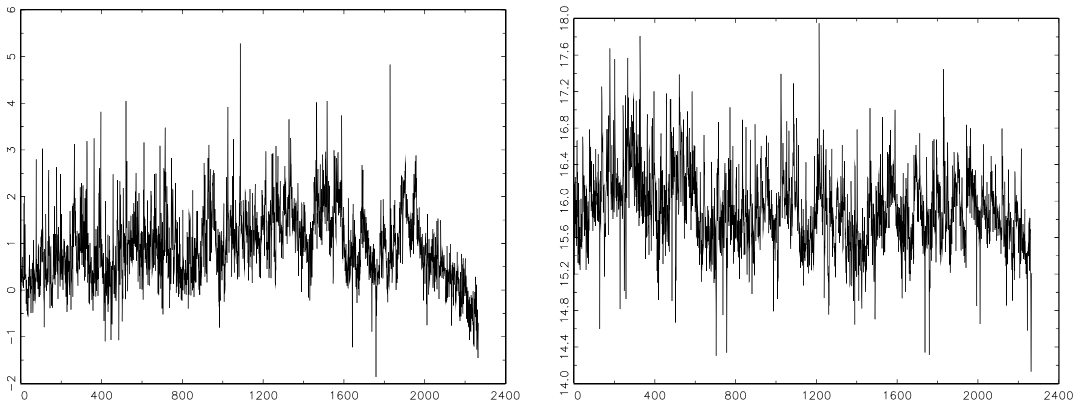

(a) $\log RV_t$ (b) $\log V_t$

Figure 1: Log-Realized volatility and Log-Volumes

(a) Nielsen and Shimotsu (2007) test

	$m_d = T^{0.5} = 48$	$m_d = T^{0.6} = 103$
d_{rv}	0.4314	0.4391
	(0.0721)	(0.0492)
d_v	0.3317	0.3476
	(0.0721)	(0.0492)
$\widehat{T}$	1.048	1.9716

(b) Cointegration rank test

	$m_L = T^{0.4} = 22$	$m_L = T^{0.5} = 48$
δ_1	0.0152	0.0106
δ_2	0.0613	0.0557
$L(u)$	$v(T) = m_L^{-0.45}$	$v(T) = m_L^{-0.35}$
$m_d = 48$,$m_L = 22$		
$L(0)$	-1.4918	-1.3109
$L(1)$	-1.3287	-1.2383
$\hat{r}$	0	0
$L(u)$	$v(T) = m_L^{-0.45}$	$v(T) = m_L^{-0.35}$
$m_d = 103$,$m_L = 48$		
$L(0)$	-1.6463	-1.4802
$L(1)$	-1.4737	-1.3906
$\hat{r}$	0	0

Table 2: Panel (a): Fractional integration estimation with exact local Whittle estimator (standard error in parenthesis). The $\widehat{T}$ test statistic is calculated with $h(T) = \log(T)$. Panel (b): Fractional cointegration estimation. The Table reports the estimated eigenvalues (δ_i) and the value of the function $L(u)$ for different choices of m and m_L.

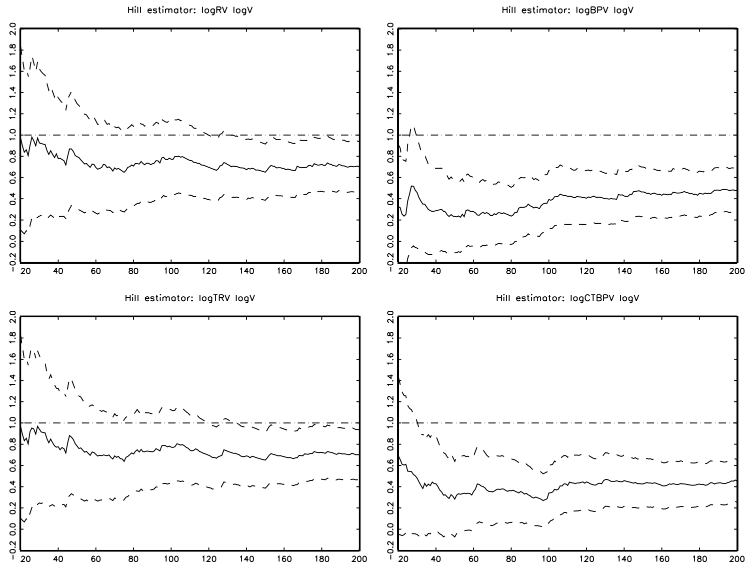

(a)

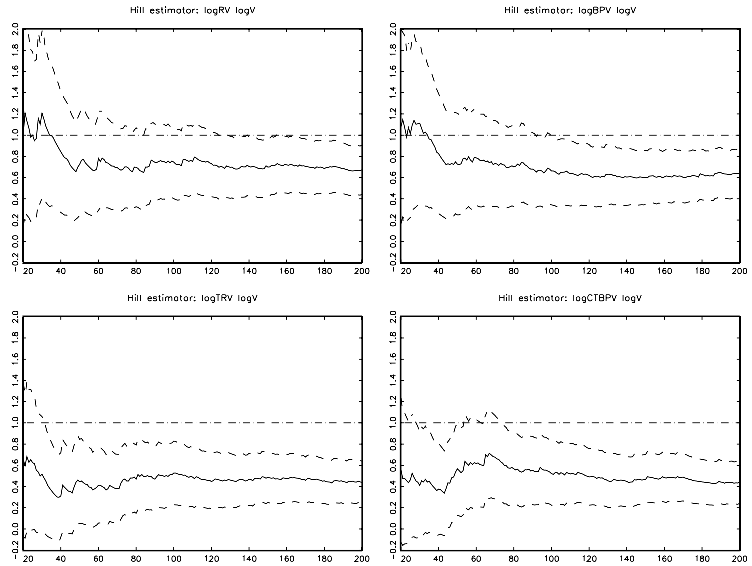

(b)

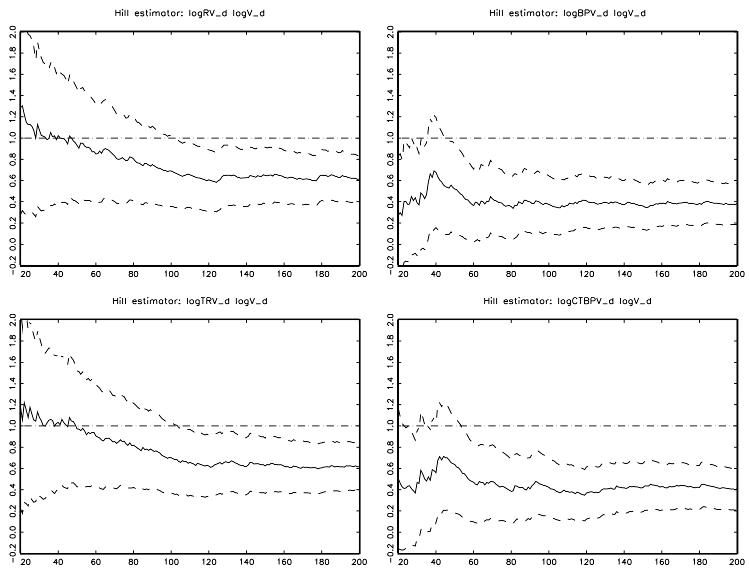

(c)

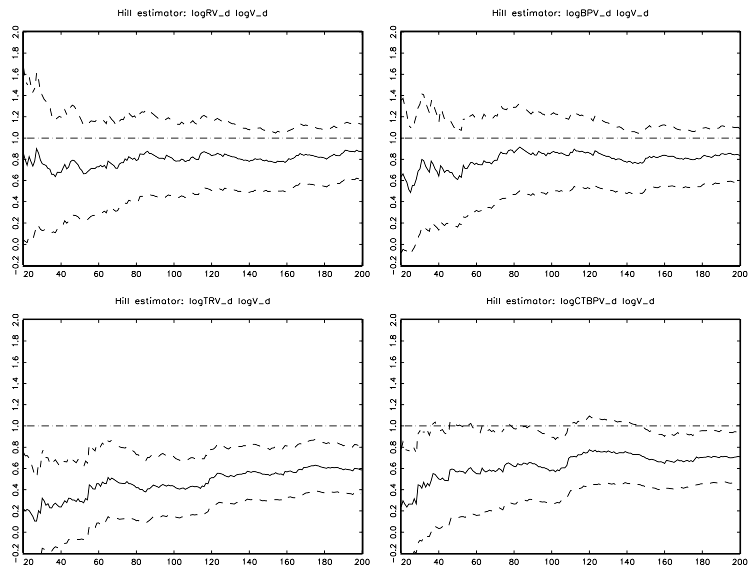

(d)

Figure 2: Panel (a) and (b) plot the Hill estimator, with the confidence bands, for left and right tails. Panel (c) and (d) reports the Hill estimator, with confidence bands, for left and right tails dependence between fractionally differenced series. The four figures in each Panel plot the Hill estimates for tail dependence between the $\log V$ and $\log RV$ (upper left), $\log BPV$ (upper right), $\log TRV$ (lower left), and $\log CTBPV$ (lower right). X-axis measures $n_u = 20, ..., 200$

	Unfiltered					Filtered				
	Right Tail					Right Tail				
	ρ	$\bar{\chi}$	$s.e.$	χ	$s.e.$	ρ	$\bar{\chi}$	$s.e.$	χ	$s.e.$
$\log RV$	0.6247	0.6700	0.2212	0.3622	0.04737	0.6143	0.7136	0.2269	0.4000	0.0523
$\log BPV$	0.6243	0.7655	0.2338	0.3306	0.0432	0.6015	0.7684	0.2342	0.3858	0.0505
$\log TVR$	0.6121	0.3682	0.1812	–	–	0.4203	0.6037	0.1862	–	–
$\log CTBPV$	0.5876	0.6253	0.2153	0.2810	0.03675	0.5682	0.6069	0.2128	0.3206	0.0419
	Left Tail					Left Tail				
	ρ	$\bar{\chi}$	$s.e.$	χ	$s.e.$	ρ	$\bar{\chi}$	$s.e.$	χ	$s.e.$
$\log RV$	0.6247	0.6961	0.2246	0.3245	0.0424	0.6143	0.9023	0.2519	0.2904	0.0380
$\log BPV$	0.6243	0.2960	0.1716	–	–	0.6015	0.4181	0.1878	–	–
$\log TRV$	0.6121	0.6954	0.2245	0.3245	0.0424	0.6037	0.9280	0.2553	0.2904	0.0380
$\log CTBPV$	0.5876	0.3395	0.1776	–	–	0.5682	0.5048	0.1993	–	–

Table 3: Tail Dependence Analysis. The Table reports the degree of positive and negative tail dependence, measured by the Hill estimator, of three different estimators of log-volatility, $\log RV$,$\log BPV$ and $\log CTBPV$, with log-volume, $\log V_t$, for unfiltered and filtered series $(1-L)^d y_t$. The parameter d is estimated with exact local Whittle estimator with a bandwidth equal to 200. The Table also reports the Pearson's ρ. The threshold, u, is chosen in order to leave on the right (left) the 2.5$\%$ of the observations.

	$NORM$	$NCOP$	$TCOP$	$GCOP$	$CCOP$	CMC	CMG
d_{RV}	0.4044^a	0.3932^a	0.3911^a	0.3966^a	0.3895^a	0.3926^a	0.3936^a
d_V	0.3765^a	0.3740^a	0.3825^a	0.3782^a	0.3822^a	0.3765^a	0.3806^a
ϕ_{11}	-0.0965^a	-0.1195^a	-0.0981^a	-0.1097^a	-0.0799^a	-0.0968^a	-0.1013^a
ϕ_{12}	0.1845^a	0.1575^a	0.1581^a	0.1731^a	0.1282^a	0.1576^a	0.1605^a
ϕ_{21}	0.0249	0.0037	0.0064	0.0043	0.0199	0.0010	0.0018
ϕ_{22}	0.1138^a	0.1014^a	0.1006^a	0.1175^a	0.0864^a	0.1014^a	0.1017^a
θ	$--$	$--$	$--$	1.6975^a	$--$	$--$	$--$
α_c	$--$	$--$	$--$	$--$	1.0661^a	$--$	$--$
ν	$--$	$--$	9.7145^a	$--$	$--$	$--$	$--$
ρ	0.6265	0.6273^a	0.6263	$--$	$--$	$--$	$--$
α_l	$--$	$--$	$--$	$--$	$--$	1.4088^a	$--$
α_r	$--$	$--$	$--$	$--$	$--$	1.2429^a	$--$
θ_l	$--$	$--$	$--$	$--$	$--$	$--$	1.8185^a
θ_r	$--$	$--$	$--$	$--$	$--$	$--$	1.6783^a
λ	$--$	$--$	$--$	$--$	$--$	0.3182^a	0.2669^a
ν_{RV}	$--$	5.5261^a	5.6359^a	6.9277^a	5.8399^a	6.2298^a	7.1068^a
ν_V	$--$	4.5594^a	4.5979^a	5.1350^a	5.4566^a	4.4122^a	4.6001^a
μ_{RV}	$--$	-0.3543	-0.3202	-0.4287^a	-0.7027	-0.4097^a	-0.4108^a
μ_V	$--$	-0.1651	-0.1322	-0.2002^a	-0.0481	-0.1410^a	-0.1520^a
σ_{RV}	$--$	0.5273	0.5168	0.5947	0.4952	0.5746^a	0.5896^a
σ_V	$--$	0.2763	0.2685	0.3051	0.2675	0.2668^a	0.2737^a
ξ_{RV}	$--$	1.0071	0.8793	1.3595^a	0.1987	1.2894^a	1.2723^a
ξ_V	$--$	0.7802	0.5781	1.0068^a	0.5900	0.6151^a	0.6849^a
$P(Q^P_{15} > q)$	0.3059	0.1759	0.2042	0.1959	0.1469	0.0663	0.0751
$P(Q^{LM}_{15} > q)$	0.2977	0.1808	0.2274	0.2111	0.1794	0.1751	0.1992

Table 4: System Estimates with different copulae densities. a,b and c stands for 1%, 5% and 10% significance level of the corresponding t-ratio test. $P(Q^P_{15} > q)$ and $P(Q^{LM}_{15} > q)$ are the p-values of, respectively, the Portmanteau test by Lutkepohl (2005) and the Breush Godfrey LM-test for autocorrelation of the residuals. $NORM$ stands for the bivariate gaussian case, $CCOP$ is the Clayton copula case, $GCOP$ is the Gumbel copula case, $NCOP$ is the normal copula case, while $TCOP$ is the t-copula case. CMC and GMC are mixture of Clayton and Gumbel copulae and are described in Appendix A.

Copula	Kendall's Tau		Tail Dependence	
$NCOP$	$\frac{2}{\pi} \cdot \arcsin(\rho)$	0.4316	0	0
$TCOP$	$\frac{2}{\pi} \cdot \arcsin(\rho)$	0.4308	$2t_{\nu+1}\left(\frac{-\sqrt{\nu+1}\sqrt{1-\rho}}{\sqrt{1+\rho}}\right)$	0.1456
$GCOP$	$1 - 1/\theta$	0.4108	$2 - 2^{1/\theta}$	0.4956
$CCOP$	$\alpha_c/(\alpha_c + 2)$	0.3477	$2^{(-1/\alpha_c)}$	0.5219

Table 5: Kendall's Tau and Tail Dependence measure.

	T_Ξ	$T_\mathbf{D}$	$S_\mathbf{B}$	S_Ξ	$S_\mathbf{D}$
$NCOP$	0.9401	1.0917*	0.4035	0.0900	0.0756*
$TCOP$	0.8864	1.0666*	0.5269	0.0802	0.1048*
$GCOP$	0.7617*	0.7623	0.5256	0.0513*	0.0648
$CCOP$	2.4144*	2.3225*	1.5325*	1.0699*	0.6234*

Table 6: Goodness-of-fit tests for alternative copula specifications: the p-values are calculated according to a bootstrap procedure. The asterisk stands for the rejection of H_0 at the 5% significance level. T_Ξ and S_Ξ are the Kolmogorov-Smirnov and Cramer-von Mises transform, respectively, of the difference between the estimated and the empirical copula. $T_\mathbf{D}$, $S_\mathbf{D}$ and $S_\mathbf{B}$ are the Kolmogorov-Smirnov and two Cramer-von Mises transforms, respectively, of the difference between the estimated and the empirical copula when applying the Rosemblatt transform (see Breymann et al. (2003) and Genest et al. (2007)).

(a) Simulated intervals for $\log RV_t$ statistics

		Clayton		Gumbel		Normal		T-copula		HAR	
Statistics	$\log RV_t$	95% Intervals		95% Intervals		95% Intervals		95% Intervals		95% Intervals	
Mean	0	-0.0867	0.2169	-0.0674	0.2513	-0.2024	0.1736	-0.1423	0.1912	-0.1472	0.1055
Std.Dev	0.7169	0.6752	0.7822	0.6784	0.7875	0.6458	0.7811	0.6718	0.7925	0.6701	0.7446
Skewness	0.6516	0.0400	0.7097	0.3172	0.8600	0.1369	1.0610	0.1638	0.9705	-0.1315	0.1280
Excess kurtosis	1.6067	0.6820	4.7980	0.6103	4.3392	0.6331	7.4001	0.6956	6.2785	-0.1900	0.2074
$q_{0.01}$	-1.4604	-1.8351	-1.3772	-1.6753	-1.2619	-1.8915	-1.3451	-1.8484	-1.3695	-0.7160	-0.6161
$q_{0.05}$	-1.0587	-1.2406	-0.8876	-1.1883	-0.8403	-1.3076	-0.9013	-1.2846	-0.8963	-0.6053	-0.4727
$q_{0.10}$	-0.8413	-0.9716	-0.6545	-0.9483	-0.6184	-1.0522	-0.6842	-1.0330	-0.6705	-1.0438	-0.7053
$q_{0.50}$	-0.054	-0.1087	0.1944	-0.1093	0.2021	-0.2113	0.1291	-0.1759	0.1552	-0.0572	0.0568
$q_{0.90}$	0.9332	0.7876	1.1431	0.8283	1.2015	0.6562	1.0890	0.7273	1.1254	0.4715	0.3409
$q_{0.95}$	1.2805	1.0746	1.4036	1.1391	1.5529	0.9539	1.4286	1.0256	1.4634	0.6169	0.7589
$q_{0.99}$	1.9777	1.6975	2.2756	1.8038	2.4019	1.6368	2.3112	1.7110	2.3073	0.8856	1.0704

(b) Simulated intervals for $\log V_t$ statistics

		Clayton		Gumbel		Normal		T-copula		HAR	
Statistics	$\log V_t$	95% Intervals		95% Intervals		95% Intervals		95% Intervals		95% Intervals	
Mean	0	-0.0932	0.1135	-0.0512	0.1411	-0.0795	0.1562	-0.0940	0.1220	-0.0583	0.0548
Std.Dev	0.4198	0.4235	0.4990	0.4116	0.4831	0.4193	0.5124	0.4307	0.5256	0.3995	0.4411
Skewness	0.2235	-0.2806	0.3986	0.2044	0.8964	-0.0324	1.2914	-0.0152	1.1953	-0.1182	0.1253
Excess kurtosis	1.1686	0.3700	3.7918	0.6194	5.3000	0.8348	10.255	0.8003	10.830	0.1996	0.2020
$q_{0.01}$	-0.9953	-1.2710	-0.9349	-1.0738	-0.7886	-1.2032	-0.8214	-1.2369	-0.9002	-1.8489	-1.5002
$q_{0.05}$	-0.6438	-0.8606	-0.6026	-0.7532	-0.5192	-0.8045	-0.5301	-0.8421	-0.5876	-1.3288	-1.0475
$q_{0.10}$	-0.488	-0.6720	-0.4435	-0.5941	-0.3877	-0.6319	-0.3873	-0.6604	-0.4348	-1.0606	-0.7972
$q_{0.50}$	-0.0153	-0.0997	0.1081	-0.0755	0.1155	-0.0900	0.1284	-0.1050	0.1033	-0.1526	0.1064
$q_{0.90}$	0.527	0.4611	0.6993	0.4888	0.7125	0.4715	0.7378	0.4608	0.7163	0.7498	1.0218
$q_{0.95}$	0.716	0.6320	0.8868	0.6686	0.9181	0.6556	0.9711	0.6499	0.9354	0.9959	1.2900
$q_{0.99}$	1.106	0.9826	1.3390	1.0694	1.4250	1.0899	1.5681	1.0758	1.5157	1.4528	1.8123

(c) Simulated intervals for the Hill's estimator

		Clayton		Gumbel		Normal		T-copula		HAR	
Tail Dependence		95% Intervals		95% Intervals		95% Intervals		95% Intervals		95% Intervals	
$\bar{\chi}_{left}$	0.6700	-0.0793	0.4545	0.4323	1.0456	0.1867	0.8393	0.2238	0.9029	0.2074	0.7875
χ_{left}	0.3622	–	–	0.2904	0.5151	–	–	–	–	–	–
$\bar{\chi}_{right}$	0.6961	0.3918	1.1096	0.0982	0.7055	0.1895	0.8825	0.2331	0.8762	0.1876	0.7874
χ_{right}	0.3245	0.2810	0.4917	–	–	–	–	–	–	–	–

Table 7: Table reports the simulated sample statistics and Hill's estimators of $\log RV_t$ and $\log V_t$ for alternative copula functions.

(a) Simulated intervals for $\log RV_t$ statistics with mixtures of copulae

$\log RV_t$					
		Mixture Clayton		Mixture Gumbel	
Statistics	$\log RV_t$	95% Intervals		95% Intervals	
Mean	0	-0.0930	0.2141	-0.1395	0.2307
Std.Dev	0.7169	0.6591	0.7605	0.6573	0.7496
Skewness	0.6515	0.2919	0.7791	0.2274	0.7571
Excess kurtosis	1.6067	0.5507	3.5993	0.4148	3.3281
$q_{0.01}$	-1.4604	-1.6527	-1.2996	-1.7096	-1.2664
$q_{0.05}$	-1.0587	-1.2083	-0.6136	-1.2436	-0.8483
$q_{0.10}$	-0.8413	-0.9348	-0.6327	-1.0082	-0.6306
$q_{0.50}$	-0.054	-0.1371	0.1538	-0.1657	0.1974
$q_{0.90}$	0.9332	0.7543	1.1333	0.7353	1.1393
$q_{0.95}$	1.2805	1.0552	1.4798	1.0358	1.4712
$q_{0.99}$	1.9777	1.7124	2.2787	1.6398	2.2294

(b) Simulated intervals for $\log V_t$ statistics with mixtures of copulae

$\log V_t$					
		Mixture Clayton		Mixture Gumbel	
Statistics	$\log V_t$	95% Intervals		95% Intervals	
Mean	0	-0.1183	0.0680	-0.0893	0.1287
Std.Dev	0.4198	0.4231	0.5028	0.4346	0.5190
Skewness	0.2235	0.02663	1.0960	0.1287	1.2627
Excess kurtosis	1.1686	0.8972	5.3009	0.9086	5.3097
$q_{0.01}$	-0.9953	-1.1932	-0.9110	-1.1520	-0.8707
$q_{0.05}$	-0.6438	-0.8340	-0.6136	-0.7811	-0.5819
$q_{0.10}$	-0.4880	-0.6718	-0.4640	-0.6323	-0.4177
$q_{0.50}$	-0.0153	-0.1380	0.0541	-0.1046	0.1012
$q_{0.90}$	0.5270	0.4184	0.6932	0.4671	0.7221
$q_{0.95}$	0.7160	0.5900	0.9059	0.6687	0.9373
$q_{0.99}$	1.1060	1.0373	1.4201	1.1130	1.5712

(c) Simulated intervals for the Hill's Estimator

		Mixture Clayton		Mixture Gumbel	
Statistics		95% Intervals		95% Intervals	
$\bar{\chi}_{left}$	0.6700	-0.0167	1.1063	0.0849	1.0907
χ_{left}	0.3622	0.1944	0.5354	0.2338	0.4999
$\bar{\chi}_{right}$	0.6961	0.0379	1.0030	0.0980	0.9248
χ_{right}	0.3245	0.2207	0.4744	–	–

Table 8: Table reports the simulated sample statistics of $\log RV_t$ (a) and $\log V_t$ (b) with the mixture of copula specifications. Panel (c) reports the simulation intervals for the Hill's estimator.

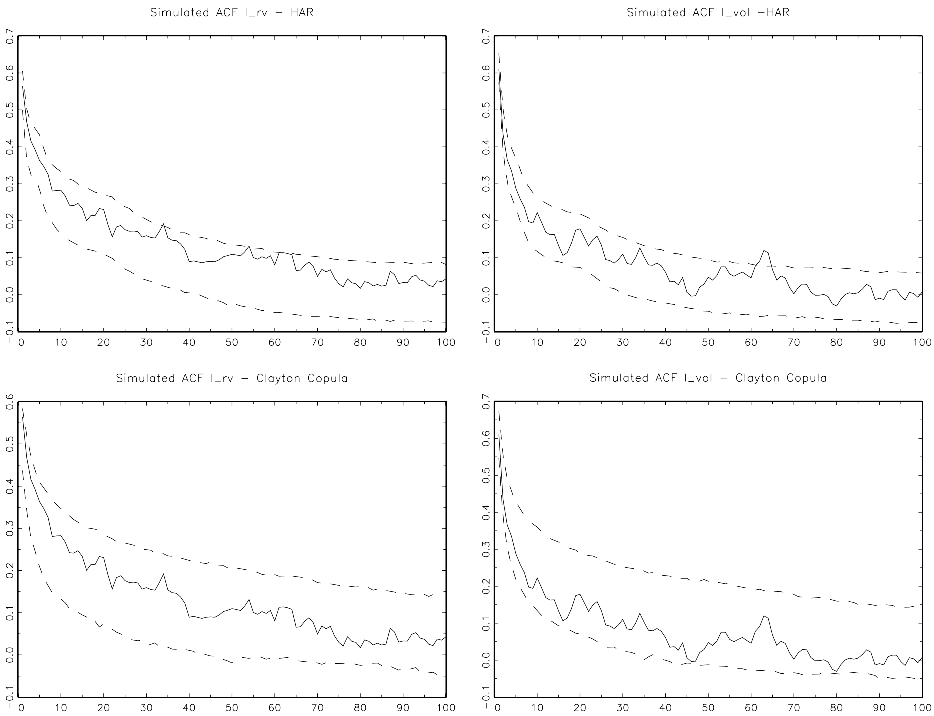

Figure 3: Simulated ACF confidence intervals of volatility and volumes.

Research Papers 2009

CREATES
Center for Research in Econometric Analysis of Time Series